RBRH

*Revista Brasileira de Recursos Hídricos*
*Brazilian Journal of Water Resources*
*Versão On-line ISSN 2318-0331*
*RBRH*, Porto Alegre, v. 25, e21, 2020
*Scientific/Technical Article*

*https://doi.org/10.1590/2318-0331.252020190050*

# Comparative study between turbulence models in curved channels

## *Estudo comparativo entre modelos de turbulência em canais curvos*

**José Rodolfo Machado de Almeida**[1] **& José Junji Ota**[1]

[1]Universidade Federal do Paraná, Curitiba, PR, Brasil
E-mails: ze.rodolfo@gmail.com (JRMA), ota.dhs@ufpr.br (JJO)

Received: April 18, 2019 - Revised: January 24, 2020 - Accepted: January 29, 2020

## ABSTRACT

This paper presents a comparative study between results obtained in two-dimensional computational simulations performed with three different turbulence models: constant viscosity; Elder Model and $k-\varepsilon$ Model. The simulations were performed using the software Telemac 2D. These results were compared to data obtained from a study in experimental channel with trapezoidal cross-section and composed of straight stretches and curves. The main objective of this comparison is to explore how turbulence models affect the general behavior of the simulated flow. To support these comparisons, statistical analysis were adopted to quantify the differences between the velocity fields obtained in the simulations and that observed in the experimental channel. The results showed that, despite the theoretical limitations, the use of the simpler turbulence closure model, that is the constant turbulent viscosity, can lead to results as good as or better than those obtained with more sophisticated models.

**Keywords:** Turbulence; Turbulence models; Two-dimensional numerical simulations; Velocity field.

## RESUMO

Este artigo apresenta um estudo comparativo entre os resultados obtidos em simulações numéricas computacionais bidimensionais realizadas com três diferentes modelos de turbulência: o de viscosidade turbulenta constante; o modelo tipo Elder; e, o modelo $k-\varepsilon$. Para a realização dessas simulações foi utilizado o software Telemac 2D. Esses resultados foram comparados com os obtidos em um estudo em canal experimental de seção transversal trapezoidal e constituído por trechos retos e por curvas. O objetivo principal dessa comparação é explorar como os modelos de fechamento de turbulência atuam na modificação do comportamento geral do escoamento simulado. Para subsidiar essas comparações adotaram-se testes estatísticos que buscaram quantificar as diferenças entre os campos de velocidades obtidos nas simulações e o observado no canal experimental. Os resultados obtidos mostraram que, apesar das limitações teóricas existentes e a dificuldade em se determinar os parâmetros de calibração, a utilização do modelo de fechamento de turbulência mais simples, pode conduzir a resultados tão bons ou melhores que os obtidos com os modelos mais sofisticados, como, por exemplo, o modelo $k-\varepsilon$.

**Palavras-chave:** Turbulência; Modelos de turbulência; Simulações numéricas bidimensionais; Campo de velocidades.

## INTRODUCTION

Numerical hydrodynamic models are important tools for predicting the behavior of watercourses, allowing the development of different environmental studies, such as the dispersion of pollutants. These models can also be used to assist the engineering project design such as water supply reservoirs, hydroelectric power plants and waterways. Although the importance of these models is notorious, the simulation of turbulent flows with the use of the Navier-Stokes equations such as they are, exceeds the processing capacity of current computers. This difficulty comes from the need to perform the simulations at the smallest scales of the flow, where the viscous effects occur, a very small discretization in space and time would be necessary.

One way to avoid this problem is to do a mathematical simplification in the Navier-Stokes equations by separating the flow into a large-scale portion (or "mean flow"), solved by using the Reynolds equations (or RANS, as usually denominated in the bibliography) and another small scale portion, or "fluctuations", in which only its overall effects on the mean flow are considerate. In this sense, Reynolds proposed an approach by which it is possible to calculate the mean flow characteristics rather than details of turbulent fluctuations. Through this approach, the characterization of a three-dimensional flow is done by use the of four equations: the Reynolds equations for the 3 dimensions and the mass conservation equation. However, this equation system is open, meaning that there are more variables than the number of equations available for its solution. The variables in this equation system are: the three components of velocity, the pressure, and the six Reynolds stresses. This fact, known in literature as the closure problem of the equations, does not allow the determination of the characteristics of the mean flow, unless the effects caused by the Reynolds stresses in the mean flow can be determined in some alternative way (Pope, 2000).

To overcome the closure problem, it is necessary to implement turbulence model. For Launder & Spalding (1972), a turbulence model consists of a set of equations that, when solved together with the mean flow equations, allows the simulation of the important aspects of Reynolds stresses in the mean flow motion, reducing the number of variables at the mean flow equation system (RANS equations). Several turbulence models are available nowadays, being the most common those that use the concept of turbulent viscosity. This concept was first proposed by Boussinesq, by associating the tangential stress arising from the turbulent fluctuations (or apparent stresses) with the Stokes law for the molecular viscosity.

These models can be classified into three groups (Friedrich, 2004). The first group contains the algebraic models, which intends to reproduce the turbulent viscosity $\nu_t$ through algebraic equations. These equations, in general, consider the multiplication of a velocity scale by a length scale, resulting in the same dimension of the kinematic viscosity ($\nu_t$) according to (Pope, 2000). The most important models in this group are the Prandtl Mixing Length (Schlichting, 1968) and the Von Karman Mixing Length (Schlichting, 1968). There are also various models that relate turbulent viscosity with speed and length scales, such as the Elder model (Launder & Spalding, 1972).

The second group is comprised of models that consider the transport of the Reynolds stresses through the computational domain done directly by the mean flow. In this kind of model, the concept of turbulent viscosity is not involved neither is the Prandtl premise, which states that turbulent fluctuations are proportional to the velocity gradient. In order to allow the use of this kind of model, it is necessary to create simplified ways to relate the transport of the Reynolds stresses to the mean flow characteristics. Another possible way to solve these models is to use additional differential equations into their formulation and solve them until certain time and space scale (discretization) from which algebraic formulas are induced in order to permit the closure of the set of equations (Eiger, 1989).

The correct application of turbulence models in numerical simulations is not trivial. It not only requires an extensive knowledge of the physical phenomena of the turbulence, but also depends on the correct choice of the appropriate model for each case. Furthermore, calibration parameters must be properly set. However, practical information that could be used to choose and calibrate those turbulence models are scarce in the literature, making it even more difficult to correctly apply them in real engineering cases.

In this sense, this paper has the main objective of contributing to the understanding of the turbulence phenomenon and the exploration of how turbulence models act in the modification of the general behavior of the simulated flow. For this, a comparative study between the results obtained in two-dimensional numerical simulations performed with the use of several formulations for the reproduction of the turbulence is presented. The comparisons presented in this paper are limited to simulations performed by a 2DH computational hydrodynamic model. These results from the computational simulations were compared to each other and to the flow observed in an experimental channel, built at the Prof. Parigot de Souza Hydraulic and Hydrology Center (CEHPAR), studied by Yamakawa (2015). The main focus of these comparisons was the velocity field in the region of the channel's curves due to the fact that the flow presents significant circulation at that location, which demands a correct choice and implementation of the turbulence model in order to simulate them in numerical models.

Although the analyses carried out in this paper is limited to Telemac 2D depth average models, the knowledge of how the turbulence models affect the results of a simulation is fundamental to improve the use of other more sophisticated CFD softwares, like, for example, Flow3D, Fluent.

## LITERATURE REVIEW

According to Launder & Spalding (1972) and Pope (2000), the choice of the turbulence model to be used in a simulation should be based on the level of detail required for the simulation, in regards to the turbulent flow characteristics; the applicability of the model to reproduce the physical phenomenon; the universality of the model; the accuracy of the results; the computational cost and facility of its application. Thus, according to Launder & Spalding (1972), the best model depends on the characteristics of the flow to be simulated and degree of knowledge prior to its simulation. It is also recommended that the choice of model should be re-evaluated if the benefit from using more a complex

model does not imply in significant gains in terms of accuracy and flexibility.

The choice of the turbulence model to be adopted in a given study can also be based on the analysis of the results obtained in similar cases. In this sense, the knowledge of existing cases in the literature has a fundamental importance in the decision on which model to use. Thus, this chapter presents a review of existing works in the literature and on the limitations and applicability of some turbulence models, with focus on curved channels.

Most of the turbulence model studies are based on the comparison of the flow characteristics in numerical simulations with experimental studies. In these cases, due to the great dependence of the geometry, it is often difficult to directly apply the conclusions obtained to different cases from those indicated in the original researches.

Indeed, the desire to compare the performance of various models of turbulence is not new. In 1973, Launder et al. (1973) developed a comparative study of the performance of six turbulence models on the reproduction of a free shear flow. These six models were separated into three groups according to their level of complexity. The models compared were:

- Turbulence models with algebraic equations: In this group are the classical mixing length models and the Prandtl's turbulent energy model;
- Turbulence models that reproduce the mixing length through differential transport equation: In this group are the classic $k-\varepsilon$ model and the extended $k-\varepsilon$ model;
- Models in which the shear stresses are the dependent variable of a conservation differential equation: in this group are the models $\overline{uv}k-\varepsilon$ and Reynolds stresses model;

Launder et al. (1973) concludes that the more sophisticated models (groups 2 and 3) had showed to be more efficient in the reproduction of different types of flow. However, no significant advantage was observed in the adoption of the Prandtl's turbulent energy model in comparison to algebraic models. Launder et al. (1973) emphasizes that the addition of the second partial differential equation in the Prandtl's turbulent energy model ($k-\varepsilon$ type models) presents a significant advantage when compared with the algebraic models since they do not require the imposition of a mixing length parameter for the flow. This allows the model to reproduce flows with different turbulent characteristics occurring along the computational domain.

Many researchers have compared the performances of turbulence models in the reproduction of complex flows, such as that occurs in sharp curves. According to Nezu & Nakagawa (1993), generally two types of secondary circulation (horizontal axis circulations) occur at curves. The first one is formed due to the interaction between the pressure forces and centrifugal force generated by the sudden change in direction. This kind of circulation is not related to the turbulence since it occurs also in laminar flow. This means that its reproduction in numerical models is unrelated to the turbulence model adopted.

The other secondary circulation that occurs at curves, often located near the outer margin of the curve, is weaker and contrary than the first one. This second circulation is formed by the non-homogeneity and anisotropy of Reynolds tensions (Nezu & Nakagawa, 1993; Blanckaert & Vriend, 2003). For this reason, according to Demuren & Rodi (1984) and Van Balen et al. (2009), this type of flow cannot be correctly reproduced by models that consider isotropic turbulent.

The complexity of the flow in curved channels becomes apparent when it is intended to reproduce it in numerical models. Gholami, et al. (2014) developed a study to verify the efficiency of a three-dimensional computational numerical model in the reproduction of the flow along a channel with a sharp curve of 90°. The numerical modeling, for which computational mesh is indicated in Figure 1, was performed based on the Reynolds equations using a variation of $k-\varepsilon$ model, called $k-\varepsilon$ RNG. The results of the experimental channel confirm the strong influence of the secondary currents in the velocity field and in the long water line profile along the channel. Gholami et al. (2014) found two secondary currents in the region of the curve, as suggested by Blanckaert & Vriend (2003) and also by Nezu & Nakagawa (1993), which was satisfactorily reproduced by the numerical model. The behavior of the secondary currents along the curve observed in the numerical model is similar to that described by Nezu & Nakagawa (1993). The intensity of the most intense secondary current was approximately 24% of the mean channel velocity.

Another similar work was performed by Booij (2003). In this research, information obtained in an experimental channel with a 180º (U shape) curve was compared to numerical simulations based on the Reynolds equations. In these simulations, the turbulence models $k-\varepsilon$ and RSM (Reynolds Stresses Model) were used. The author found that although the average flow was well reproduced, the adoption of turbulence models based on the Reynolds concept did not allow a good reproduction of the secondary currents in the region of the curve, indicating, therefore, that the turbulent phenomena could not be correctly reproduced. After this limitation was verified, the author implemented a model based on the LES or Large Eddy Simulation approach, with the Smagorinsky turbulence model. With the use of this model, significantly better results were obtained. A discussion of the limitations on the simulation of secondary currents in curved channels by using turbulence models that consider a linear dependence between Reynolds Stresses, such as $k-\varepsilon$ model, is presented by Van Balen et al. (2009).

Wilson et al. (2002) compared the performance of three turbulence models in the prediction of the discharge curve in composite channels. It was studied both flows occurring within

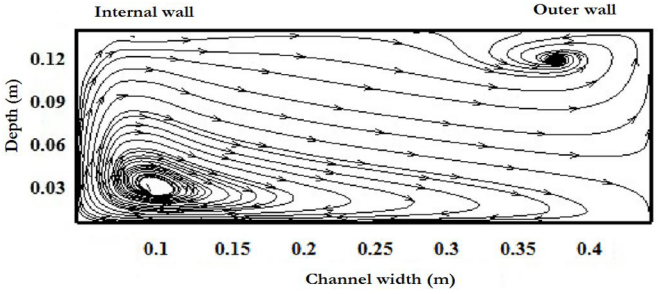


**Figure 1.** Secondary Currents downstream of the curve. Source: Adapted from Gholami et al. (2014).

the main channel and flows that occur when the flow occupies the flood plains. The characteristics of the flow in a rectilinear channel and in a meandering channel were also studied. A two-dimensional model was applied. The compared models were: (i) $k-\varepsilon$ model; (ii) Elder model, and; (iii) Constant viscosity model.

The simulations showed that the use of numerical models based on the Reynolds equations allows satisfactory prediction of the water levels for the verified conditions. It was observed, however, that the more sophisticated models, $k-\varepsilon$ model and the Elder model, had better results in comparison to the constant viscosity model. This occurred for both rectilinear and meandering channels. It was also observed that, due to the combination between the normally used mesh discretization and the existence of partially wet elements on the sidewalls of the channels, the numerical model had difficulty in the simulation of the flow behavior inside the main channel. When the flow occupies the flood plains that occur on higher discharges, all the elements of the mesh become completely wet, avoiding the problems associated with the reproduction of the velocity vectors when partial dry elements exist. In this work, it was also identified problems in the reproduction of the circulation currents along the curves of the meandering channel.

Other studies intended to identify the applicability of turbulence models through real case studies. In those studies, several simulations were performed to verify which turbulence model allows a better reproduction of the observed flow characteristics.

In this sense, the work developed by CHC (Canadian Hydraulics Centre, 2009) stands out. In this study, the characteristics of the velocity field of a section of the St. Clair River, located on the border between the state of Michigan and the Canadian state of Ontario was attempted to be reproduced. The velocities field of this stretch of the river was measured on July 2, 2003 with an ADCP (Acoustic Doppler Current Profiler). Based on these measurements, computational numerical models were developed using the Telemac 2D software. In these simulations, several turbulence models were tested in order to identify the one that best suits the field measurements. The comparisons was based only on the behavior of the velocity field verified on the river, and no statistical tests were applied.

The simulations performed by Chc (Canadian Hydraulics Centre, 2009) indicated that the Elder and Smagorinsky turbulence models were more efficient in the reproduction of circulations in the studied region. It was observed that the results obtained with $k-\varepsilon$ model showed circulating currents smaller than those observed in the field, evidencing that, for the studied case, the simulation produced a more viscous flow than desired.

## METHODOLOGY

### Velocity field mapping in the experimental channel

The results and measurements presented by Yamakawa (2015) were used for the comparison of numerical simulations results. For that study, an experimental curved channel was constructed with the geometry presented in Figure 2. As it can be observed, the experimental channel used measures 39.2 m in length and has straight sections and 8.5 m radius curves. Its' cross section has a 3 meter width base trapezoidal shape. The channel button is horizontal, positioned at a height of 0.0 cm.

The test performed by Yamakawa (2015) had the following boundary conditions: at the upstream boundary, it was imposed a constant discharge of 0.340 $m^3/s$ and at the downstream boundary a 0.2817 m depth was imposed. Analysis of the Froude and Reynolds numbers indicate that the flow is subcritical and is at the smooth-rough transition zone regime.

The general characteristics of the flow are shown in Figure 3. As it can be seen, some superficial circulation zones in the region of the curves were visually identified by using floating tracers. Figure 4 shows the regions where those circulations were observed.

The flow velocity field was measured by using an ADV (Acoustic Doppler Velocimetry). Figure 5 presents the results obtained at the cress sections. Analyzing those data it's possible to identify circulation zones (negative flow velocities) near the left margin of the channel at the sections C, D and E. Those circulations are even larger than shown in the figure because the superficial layer of the flow, where most of the circulations are located, could not be measured due to limitation of the equipment. This can be verified by the cooperation of the data of the Figure 4 and 5. It is also possible to identify the concentration of the flow at the right margin of the channel (Sections C, D, E and F).

The depth average velocities at the cross sections are indicated in Figure 6

### Numerical model simulations

The numerical simulations were performed using the Telemac 2D software, which consists of a computational hydrodynamic model, developed to reproduce free surface flows, both in subcritical regime and in supercritical regime. This program has been developed by the LNHE (*Laboratoire National d'Hydraulique et Environnement*) of the Research and Development Department of the French company Eletricité de France (Hervouet, 2007).

The computational domain was defined considering the same limits of the experimental channel. The finite element mesh was elaborated by using BlueKenue 64® software, developed by the National Research Council Canada (Canadian Hydraulics Centre, 2010). To verify the mesh elements size, a sensibility analysis based on the characteristics of the larger circulation was performed. During the analysis, it was verified that the size of the circulation does not change significantly if elements smaller than 5 cm are adopted (Figure 7). However, triangular elements with 3.0 cm edges were adopted to better reproduce the geometry of the berms of the margins. Besides, to better represent the geometry of the problem, the computational mesh was constructed in a way to guarantee the existence of nodes in the offsets of the slopes that define the channel margins. Figure 8 shows the mesh used in the simulations, which has 244,414 nodes and 485,812 elements.

As indicated in Figure 9, the discharge was imposed at the upstream section and the water level was imposed at the downstream section of the numerical model. These boundary conditions are sufficient for the reproduction of subcritical flows.

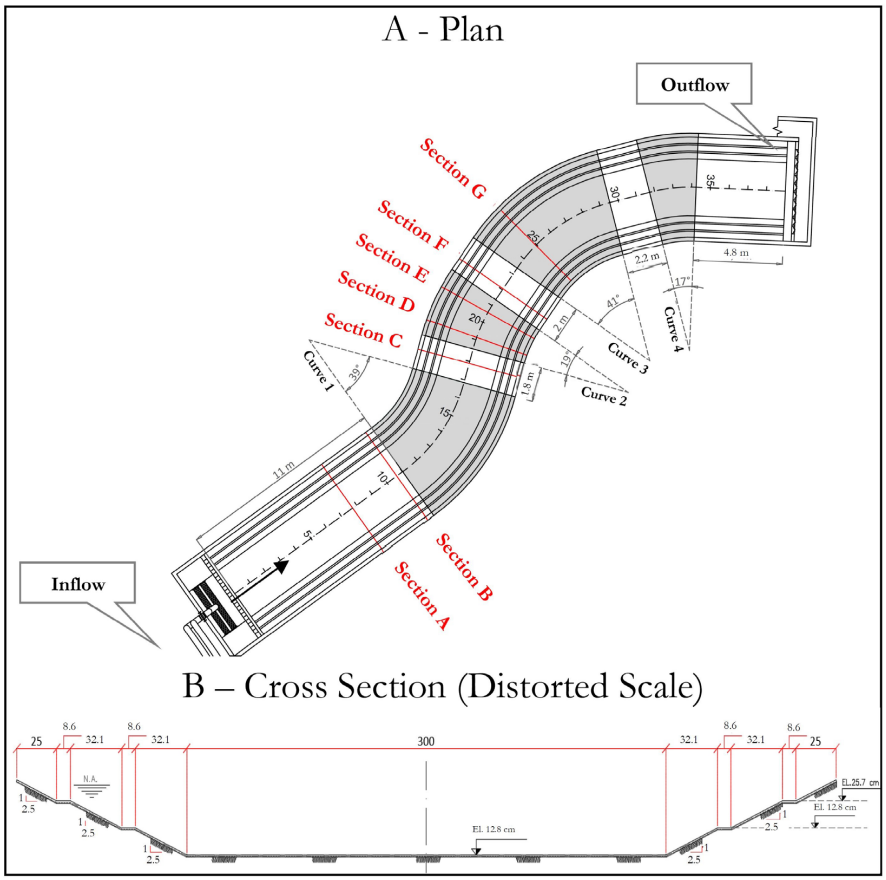


**Figure 2.** General layout of the experimental channel. Source: Adapted from Yamakawa (2015).

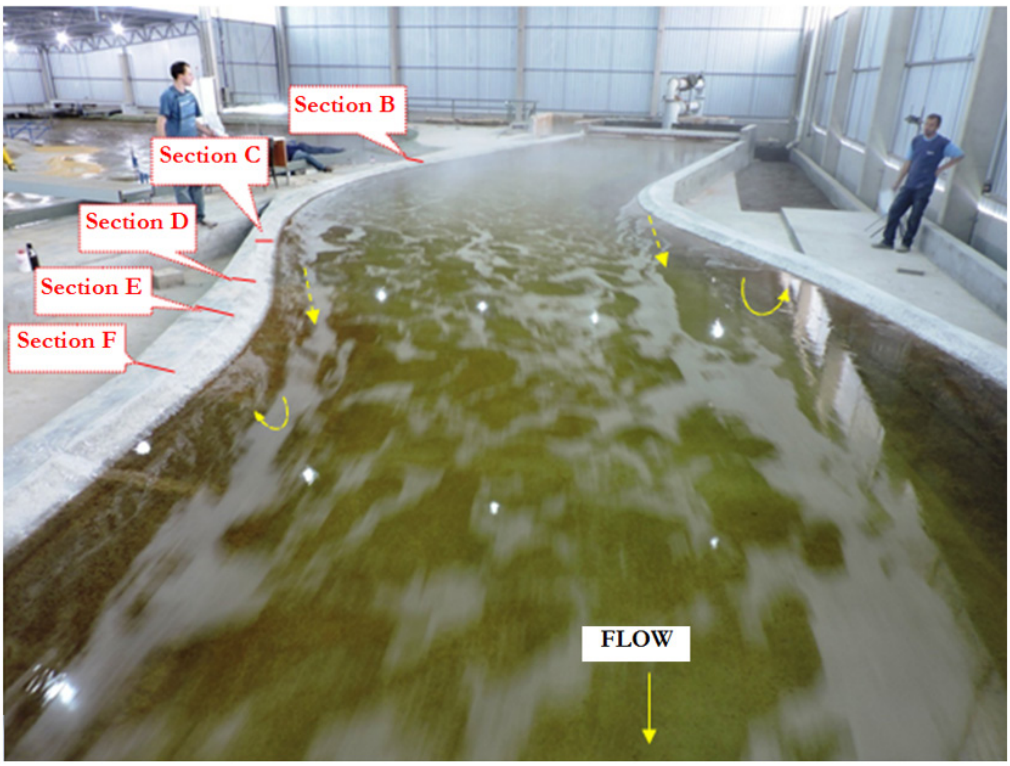


**Figure 3.** General view of the flow at the curves 1 e 2. Source: Adapted from Yamakawa (2015).

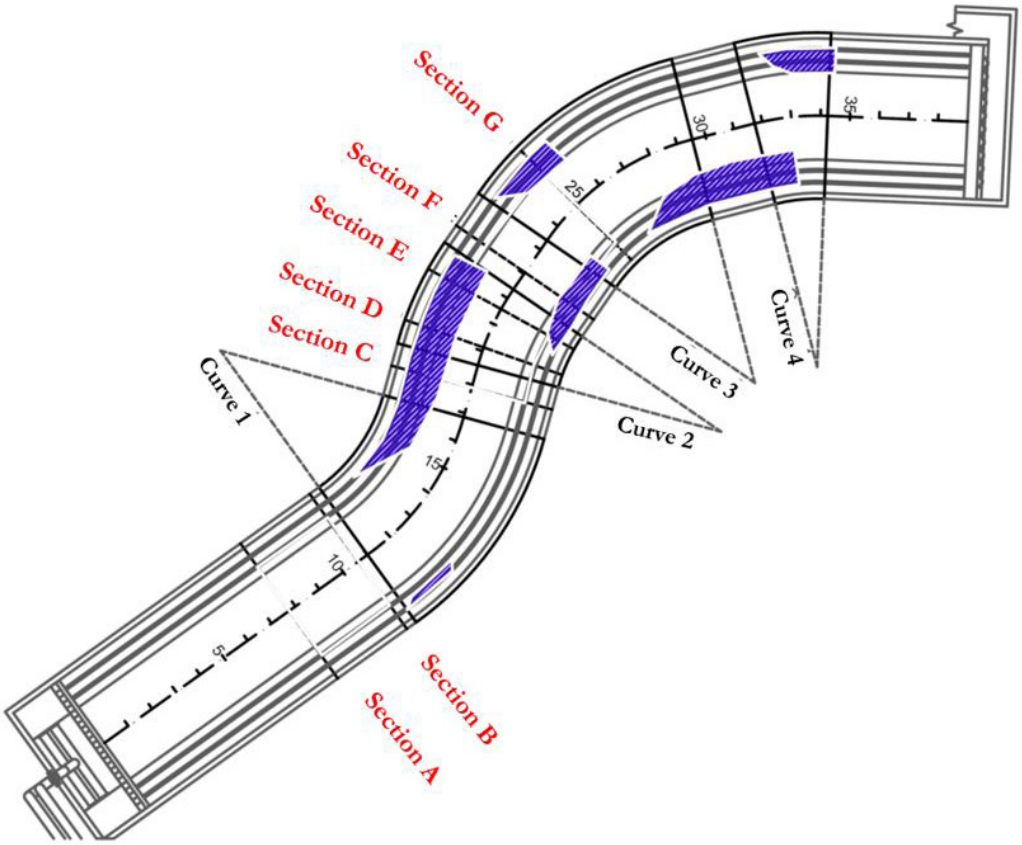


**Figure 4.** Superficial circulations observed. Source: Adapted from Yamakawa (2015).

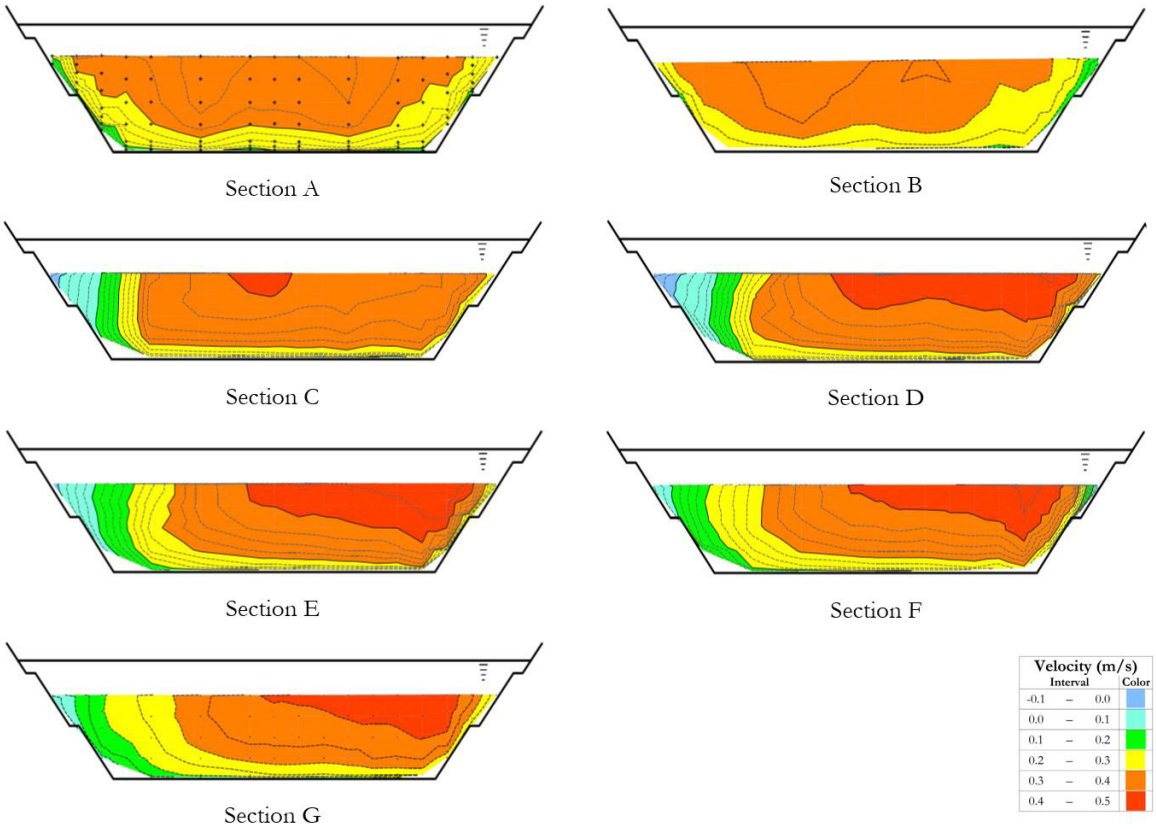


**Figure 5.** Flow velocity observed at the experimental channel. Source: Adapted from Yamakawa (2015).

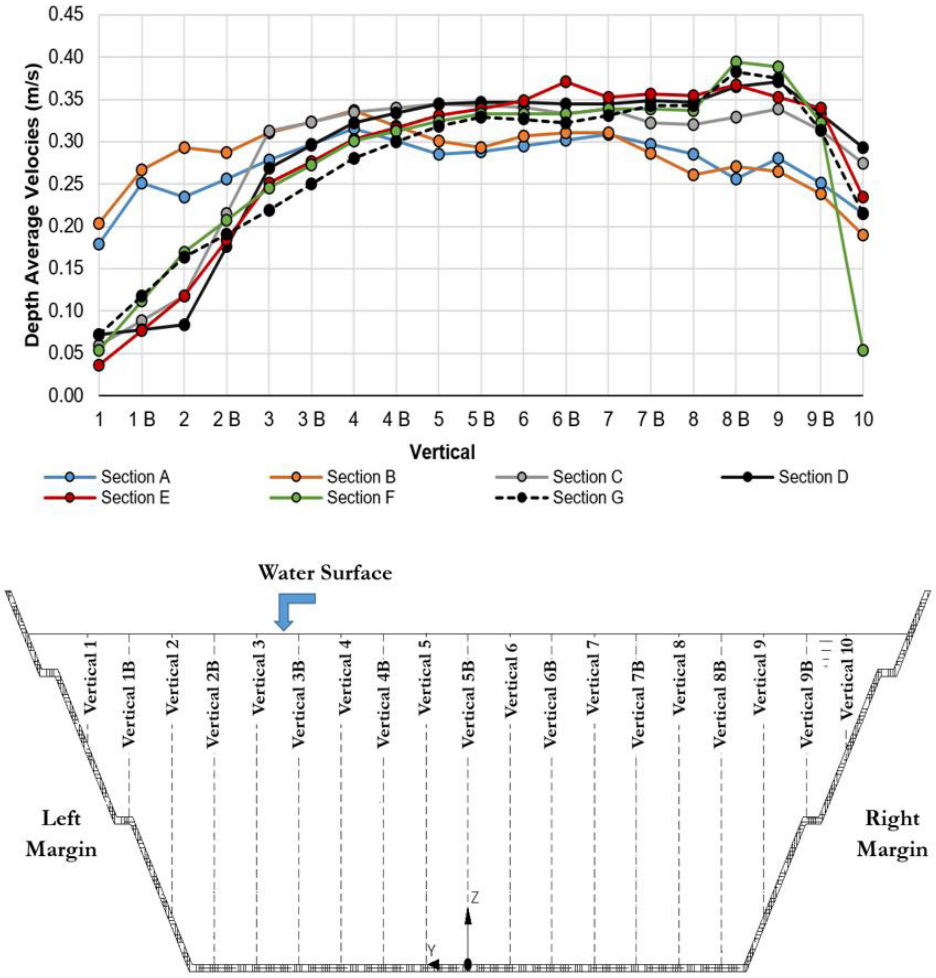


**Figure 6.** Depth Average Velocities in the experimental channel.

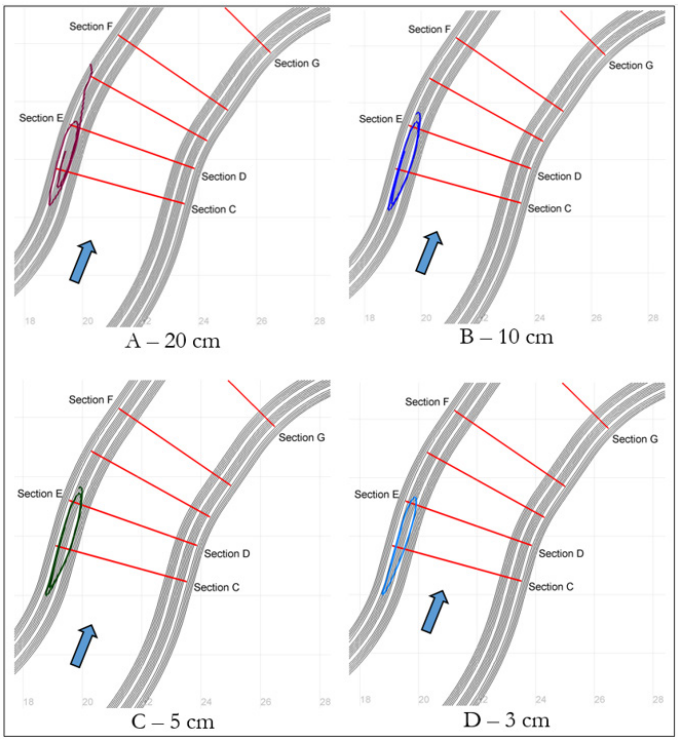


**Figure 7.** Mesh size sensibility analysis.

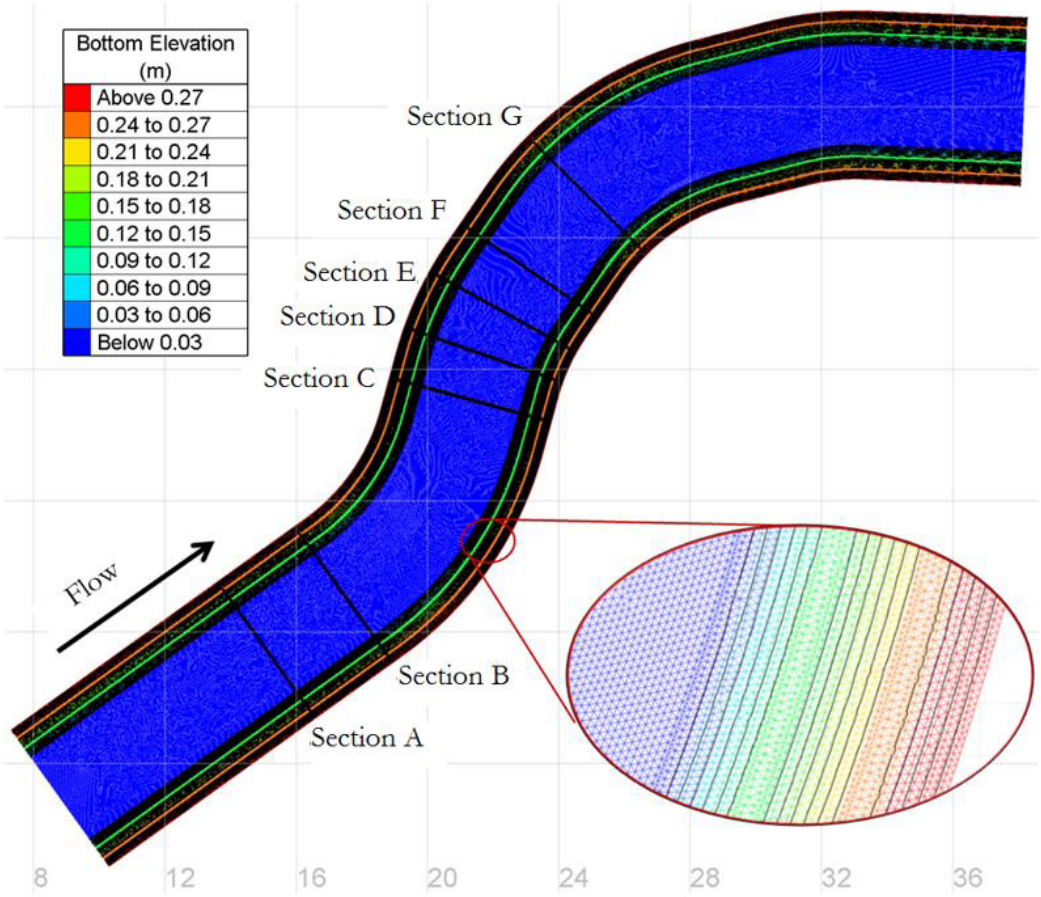


**Figure 8.** Computational domain of the numerical model.

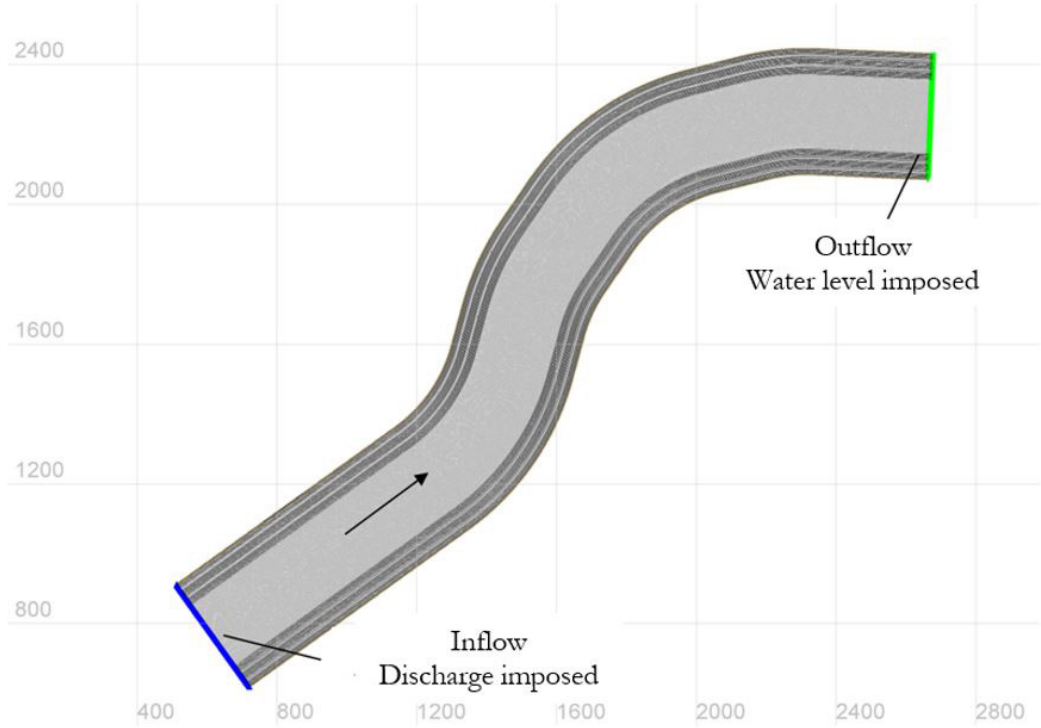


**Figure 9.** Boundary conditions at the numerical simulations.

The algorithm of the Telemac two-dimensional hydrodynamic model, version v7p1, used in the numerical simulations presented in this paper, allows the use of the following turbulence models:

- Constant viscosity model;
- Elder type model;
- $k-\varepsilon$ Model;

The simulations indicated in Table 1 were performed in this work. The time step adopted allowed a maximum Currant number of 0.4.

## Analysis of the results and comparison with the experimental velocity field

The velocity fields obtained with numerical simulations were evaluated by statistical comparison to the experimental data. This comparison was made by applying the formulations indicated below:

Mean Absolute Error (*MAE*)

The Mean Absolute Error, for which definition is given in Equation 1, can vary from zero to plus infinity, being zero the exact correspondence.

$$MAE = \frac{\sum_{i=1}^{n}|O_i - S_i|}{n} \tag{1}$$

Where $O_i$ represents the value observed in the experimental channel, $S_i$ is the simulated value in the numerical model and $n$ is the number of observations.

Average Percentage Error (*MPE*)

The Mean Percentage Error, for which definition is given in Equation 2, can vary from plus infinity to minus infinity, being zero the exact correspondence.

$$MPE = \frac{\sum_{i=1}^{n}\frac{O_i - S_i}{O_i}}{n} x100 \tag{2}$$

Average Absolute Percent Error (*AAPM*)

The Average Absolute Percent Error, for which definition is given in Equation 3, can vary from 0 to plus infinity, being zero the exact correspondence.

$$AAPE = \frac{\sum_{i=1}^{n}\left|\frac{O_i - S_i}{O_i}\right|}{n} x100 \tag{3}$$

Nash and Sutcliffe Efficiency Coefficient (*NSE*)

The Nash-Sutcliffe efficiency Coefficient (Nash & Sutcliffe, 1970), indicated in Equation 4, corresponds to the square of observed differences related to the variance of the observations. In other words, NSE indicates how well the plot of observed versus simulated data fits the 1:1 line.

**Table 1.** Performed simulations.

| Test | Turbulence Model |
|---|---|
| 1 | Constant $\nu_t$ model |
| 2 | Elder Model |
| 3 | $k-\varepsilon$ Model |

$$NSE = 1 - \frac{\sum_{i=1}^{n}(O_i - S_i)^2}{\sum_{i=1}^{n}(O_i - \bar{O})^2} \tag{4}$$

Where $\bar{0}$ represents the average of the observations in the experimental channel;

The Nash-Sutcliffe Efficiency Coefficient can vary from minus infinity to 1 with 1 being the exact correspondence of the simulated data to the observed data and minus infinity indicating that the analyzed values has no correspondence. Thus, the classification indicated in Table 2 can be used as a reference to classify the efficiency of a model.

Among the advantages of the use of the NSE coefficient it can be highlighted that it is an ASCE recommendation and it is very commonly used, which provides extensive information on reported values (Moriasi et al., 2007).

# RESULTS AND DISCUSSION

## Estimation of the turbulent flow viscosity in the experimental channel

The variation of the turbulent kinetic viscosity can be obtained by using Equation 4. This equation originates from the comparison of the Boussinesq approximation with the turbulence model proposed by Von Karman and assuming a linear distribution of the shear stresses along the vertical of the flow.

$$\nu_t = \kappa \nu_* y\left(1 - \frac{y}{y_0}\right) \tag{5}$$

Where $\nu_t$ is the turbulent kinematic viscosity [$L^2\ T^{-1}$], $\kappa$ the von Karman constant [-], $\nu_*$ the shear velocity [$LT^{-1}$], $y$ the vertical distance measured from the bottom [L] and $y_0$ the flow depth [L].

The average turbulent viscosity of the flow can then be estimated from Equation 6:

$$\overline{\nu_t} = \frac{1}{y_0}\int_0^{y_0}\nu_t dy \tag{6}$$

Thus:

$$\overline{\nu_t} = \frac{\nu_* y_0}{15} = 0{,}0667\,\nu_* y_0 \tag{7}$$

This value is similar to the minimum value for the β coefficient of the Equation 8 suggested by Wilson et al. (2002). However, Wilson et al. (2002) mentions that the coefficient β can be significantly higher depending on the general characteristics of the flow, being, for symmetrical channels, up to 0.27.

$$\nu_t = \beta \nu_* h \tag{8}$$

**Table 2.** Classification of the model through ht NSE coefficient.

| Classification | Value of the coefficient NSE |
|---|---|
| Very good | 0.75 < NSE < 1.00 |
| Good | 0.65 < NSE < 0.75 |
| Acceptable | 0.50 < NSE < 0.65 |
| Not acceptable | NSE < 0.5 |

Thus, considering the general flow characteristics observed by Yamakawa (2015) for the experimental channel, the value of the turbulent kinematic viscosity can vary, as indicated in Equation 9.

$$440\ \nu < \nu_t < 1800\ \nu \quad (9)$$

Where $\nu$ is the kinematic viscosity of water, which is of the order of $10^{-6}$ m$^2$/s.

## Test 1 - constant viscosity model

The turbulence model with constant viscosity is the simplest model studied in this research. In this model, the turbulent viscosity is considered constant throughout the computational domain, independently of the characteristics of the flow or the chosen spatial and temporal discretization. It is also implied that turbulence is not propagated along the flow, i.e. it is dissipated in the same region in which it is produced.

According to Equation 9, the turbulent kinematic viscosity of the flow in the analyzed channel should be of the order of $10^{-3}$. For the evaluations performed in this work, 4 simulations were made, whose turbulent viscosity values are indicated in Table 3. The physical interpretation of these values indicates that the diffusion of the flow properties, such as momentum and concentration of suspended solids are much more influenced by the characteristics of the fluctuations (turbulence) of the flow (which is of the order of $10^{-6}$ m$^2$/s).

Figure 10 summarizes the flow characteristics observed in simulations 1-A and 1-D. As it can be seen, an increase in turbulent viscosity decreases the intensity of the separations occurring in the region of the curves. For simulation 1-A, performed with turbulent viscosity equal to 0.1 m$^2$/s, these separations were practically non-existent, which is evidenced by the approximately symmetrical distribution of velocities along the cross-sections. With the decrease in turbulent viscosity, a progressive increase in the intensity of the separations can be seen, making the geometry of the contour more important in the definition of the velocity field.

As shown in Figure 10, in the 1-D simulation circulations occur both at the left margin, immediately downstream of curve 1, and at the right margin, downstream of curve 2. This same behavior was observed in the experimental channel (Figure 4). It was also possible to observe that the flow concentration near the right margin at the region of the curves is similar to experimental observations, with flow velocity above 0.4 m/s. Figure 11 presents the comparison between the depth average velocity at the sections D and F at the experimental channel and at the simulation 1-D. It can be seen that the numerical model reproduced the general behavior of the flow.

**Table 3.** Test 1 – Simulations performed.

| Simulation | Turbulent viscosity (m$^2$/s) |
|---|---|
| 1 – A | $\nu_t = 10^{-1}$ |
| 1 – B | $\nu_t = 10^{-2}$ |
| 1 – C | $\nu_t = 5 \times 10^{-3}$ |
| 1 – D | $\nu_t = 10^{-3}$ |

Table 4 summarizes the statistical evaluations performed. The evaluations presented in this table confirm that a lower value of turbulent viscosity shows results with a higher compatibility to the experimental data. However, contrary to what was expected, the statistical evaluations showed that the simulation made with the turbulent viscosity of $10^{-3}$ m$^2$/s did not present the best results. The simulation with the most adherent results to the experimental data was the one performed with a turbulent viscosity of 0.005 m$^2$/s. A possible explanation for this unexpected behavior is the appearance of a more intense circulation downstream of curve 1 for Test 1-D.

## Test 2 - Elder model

The Elder model (Elder, 1959) uses two algebraic equations for the determination of turbulent viscosity. In this model, the turbulent viscosity is estimated from the mean flow characteristics, as indicated in Equations 10 and 11. Although it is a more sophisticated model than the model with constant turbulent viscosity, the Elder Model has an important limitation: the source of the turbulence is local, that is, the fluctuations that occur in one position are generated in the same place.

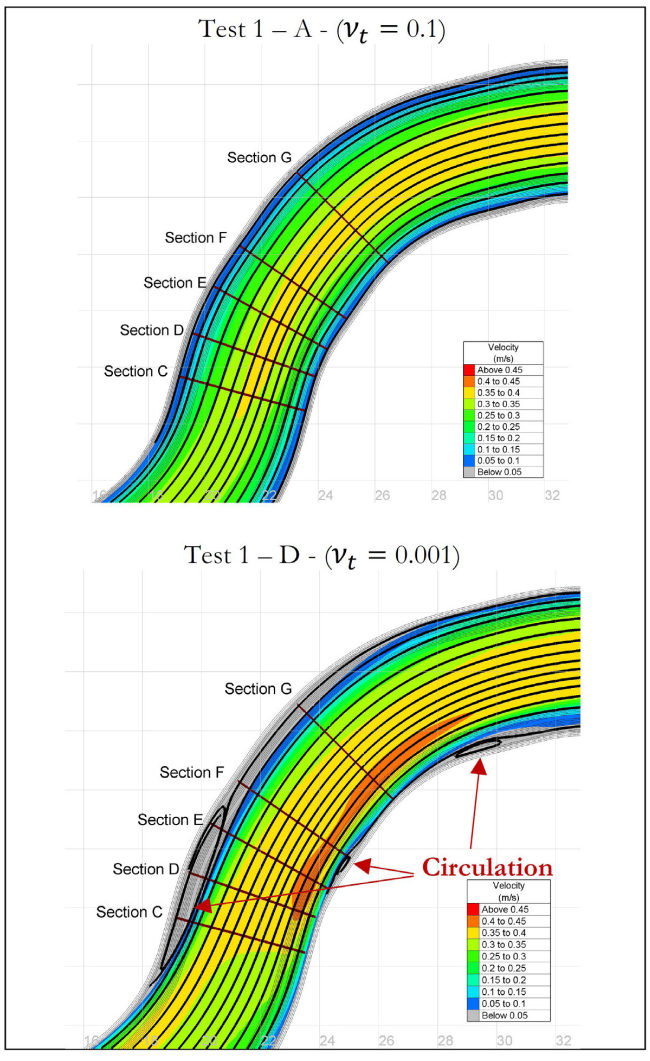


**Figure 10.** Test 1 – Streamlines.

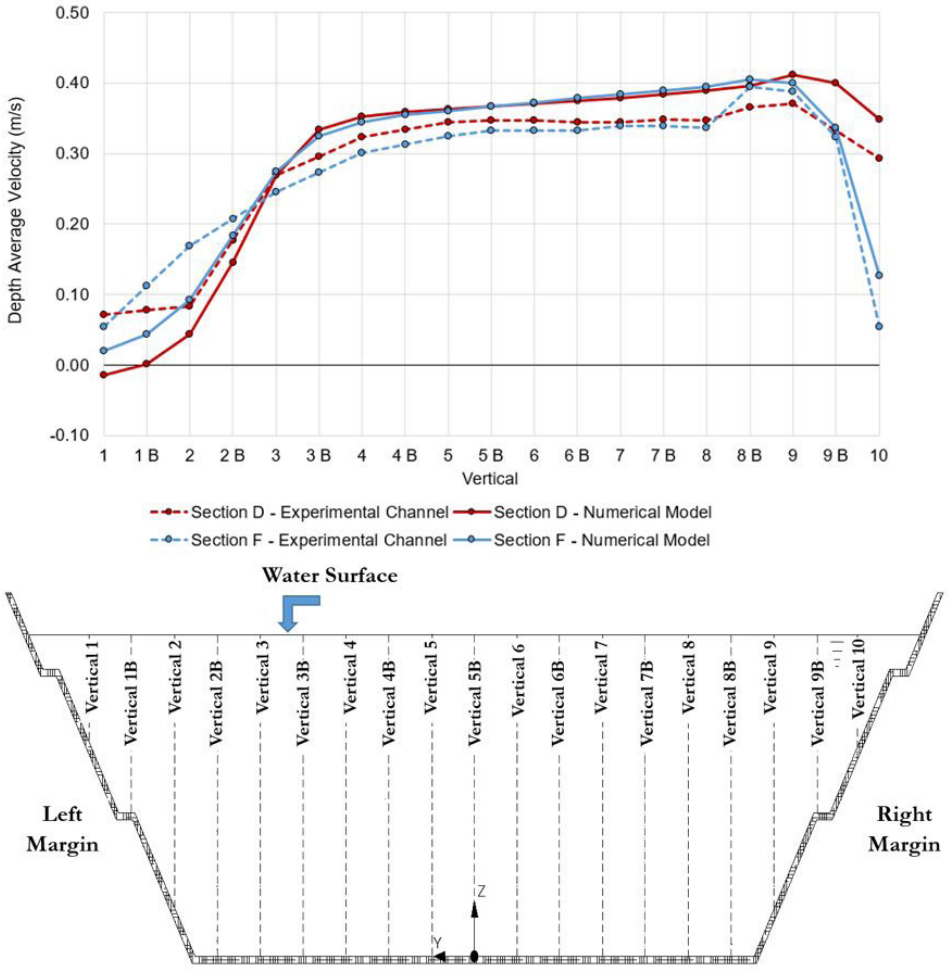


**Figure 11.** Test 1-D –Depth average velocity.

**Table 4.** Test 1 – Statistical characterization.

| Statistical evaluation | Test 1 ($\nu_t$ = 0.1) | Test 2 ($\nu_t$ = 0.01) | Test 3 ($\nu_t$ = 0.005) | Test 4 ($\nu_t$ = 0.001) |
|---|---|---|---|---|
| **MPE** | **0.87** | 5.88 | 5.55 | 0.96 |
| **MAE** | 0.041 | 0.034 | **0.028** | 0.036 |
| **AAPE** | 19.35 | 14.05 | **12.19** | 18.80 |
| **NSE** | 0.28 | 0.52 | **0.84** | 0.80 |

$$\nu_{tt} = \alpha_t \nu_* h \quad (10)$$

$$\nu_{tl} = \alpha_l \nu_* h \quad (11)$$

At the equations, $\nu_{tt}$ represents the transversal turbulent viscosity, $\nu_{tl}$ the longitudinal turbulent viscosity, $\alpha_t$ the transversal dispersion coefficient, $\alpha_t$ the longitudinal dispersion coefficient and $\nu_*$ the shear velocity.

Equations 10 and 11 show that Elder model considers separately the turbulence in the longitudinal and transversal direction of the flow. Telemac 2D allows the operator to choose the dimensionless parameters to be used in each direction.

For this research, 4 simulations were performed, as shown in Table 5. In these simulations, the coefficient $\alpha_t$ was changed while the coefficient $\alpha_l$ was kept constant with the value recommended by the bibliography. This procedure was adopted because the dissipation in the longitudinal direction of the flow tends to be less important in the development of the circulations in the region of the curves, which are the focus of this study.

**Table 5.** Test 2 – Simulations performed.

| Simulation | Dimensionless parameters used |
|---|---|
| 2 – A | $\alpha_l$ = 6.0 ; $\alpha_t$ = 0.2 |
| 2 – B | $\alpha_l$ = 6.0 ; $\alpha_t$ = 0.6 |
| 2 – C | $\alpha_l$ = 6.0 ; $\alpha_t$ = 1.0 |
| 2 – D | $\alpha_l$ = 6.0 ; $\alpha_t$ = 2.0 |

It is evident in Figure 12 that a decrease in the transverse dispersion coefficient significantly increases the regions where separations occur and move them downstream. It is also verified that the larger circulations for the tests with lower values of

dispersion coefficient affect the flow velocity in the region of the curves. That occurs because the larger circulations reduce the effective flow area, increasing the concentration of flow at the right margin.

Figure 12 shows the velocity field obtained in simulation 2-A, performed with the coefficient $\alpha_t$ = 0.2. As it can be seen, the circulation near the left margin, in the region of the curves, extended to the region located between sections F and G. With the increase

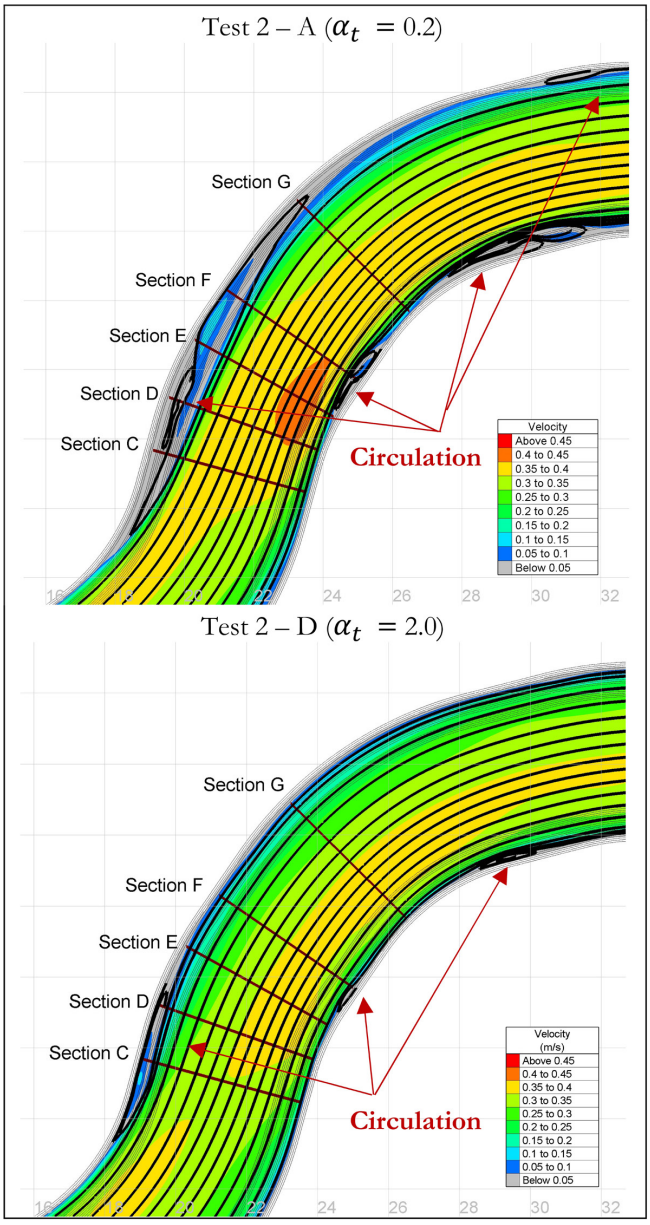


**Figure 12.** Test 2 – Streamlines.

**Table 6.** Test 2 – Statistical characterization.

| Statistical evaluation | Test 2-A $\alpha_t$ = 0.2 | Test 2-B $\alpha_t$ = 0.6 | Test 2-C $\alpha_t$ = 1.0 | Test 2-D $\alpha_t$ = 2.0 |
|---|---|---|---|---|
| **MPE** | -5.96 | **1.96** | 8.04 | 18.43 |
| **MAE** | 0.044 | 0.034 | **0.032** | 0.029 |
| **AAPE** | 26.35 | 20.26 | **19.13** | 20.12 |
| **NSE** | 0.78 | **0.80** | 0.78 | 0.64 |

of the dispersion coefficient it was observed that the circulations present a clear tendency of decreasing, being reduced to a very small area for the test with the coefficient $\alpha_t$ = 2.0. Comparing the result of the simulation 2-D to experimental data (Figure 4), it is verified that the regions where the circulations occur are larger in the experimental channel, which indicates that the dispersion coefficient used in simulation 2-D may be high than necessary.

As can be seen in Table 6, simulations 2-B and 2-C have the best performance compared to the experimental data. The analysis of the results from the MPE (Mean Percent Error) and NSE (Nash Efficiency Coefficient) indicate that the best parameter for the reproduction of the flow along the channel is $\alpha_t$ = 0.6, as suggested by Wilson et al. (2002). However, it is observed that the use of this dispersion coefficient caused a separation zone with more intense circulations than those observed experimentally, mostly near the left margin in the regions of the sections C, D and E.

As expected, higher dispersion coefficient causes a decrease in the circulations along the left margin of the channel. It was observed, however, that the increase in the value of the dispersion coefficient also causes an increase in the differences along the left margin in sections E, F and G, indicating a less intense circulation than the experimental observations. So, the results show that the $\alpha_t$ = 2.0 is not adequate. The adoption of this coefficient induced a turbulent viscosity greater than that observed experimentally, which caused a significant decrease of the circulations in both margins of the channel.

The difficulty encountered in minimizing the differences between the experimental and the simulated velocity field by changing the dispersion coefficients of the Elder Model may be due to the fact that this model, although more sophisticated than the constant turbulent viscosity model, still do not consider the transport of the turbulence through computational domain. Consequently, a change in the coefficient can bring benefits to one region, but it also may negatively impact the results elsewhere. This can be a especially important factor for the studied channel, given the complexity of the flow that presents circulation zones in both banks and secondary currents. These three-dimensional features cannot be adequately reproduced in a two-dimensional numerical model, regardless of the turbulence closure scheme adopted.

Figure 13 presents comparisons of the depth average velocity at the experimental channel and the simulations 2- A and 2-D. For the simulation 2-A, the circulations near the left margin was more intense than desired (experimental channel with greater velocity). The opposite occurs for the simulation 2-D.

## Test 3 - $k-\varepsilon$ model

$K-\varepsilon$ model is the most sophisticated turbulence model among those studied in this work. As presented by Wilcox (1994) and Eiger (1989), this model uses two differential equations in its formulation, one of them for the reproduction of turbulent kinetic energy $k$ and the other to reproduce the energy dissipation rate $\varepsilon$. The principal advantage of this kind of model is that, once they use a more general formulation, it is not necessary to introduce a value for the mixing length $l_m$. Another advantage of this model is that, by using differential equations, the $k-\varepsilon$ model allows the transport of the characteristics related to the production and dissipation of the turbulence along the computational domain.

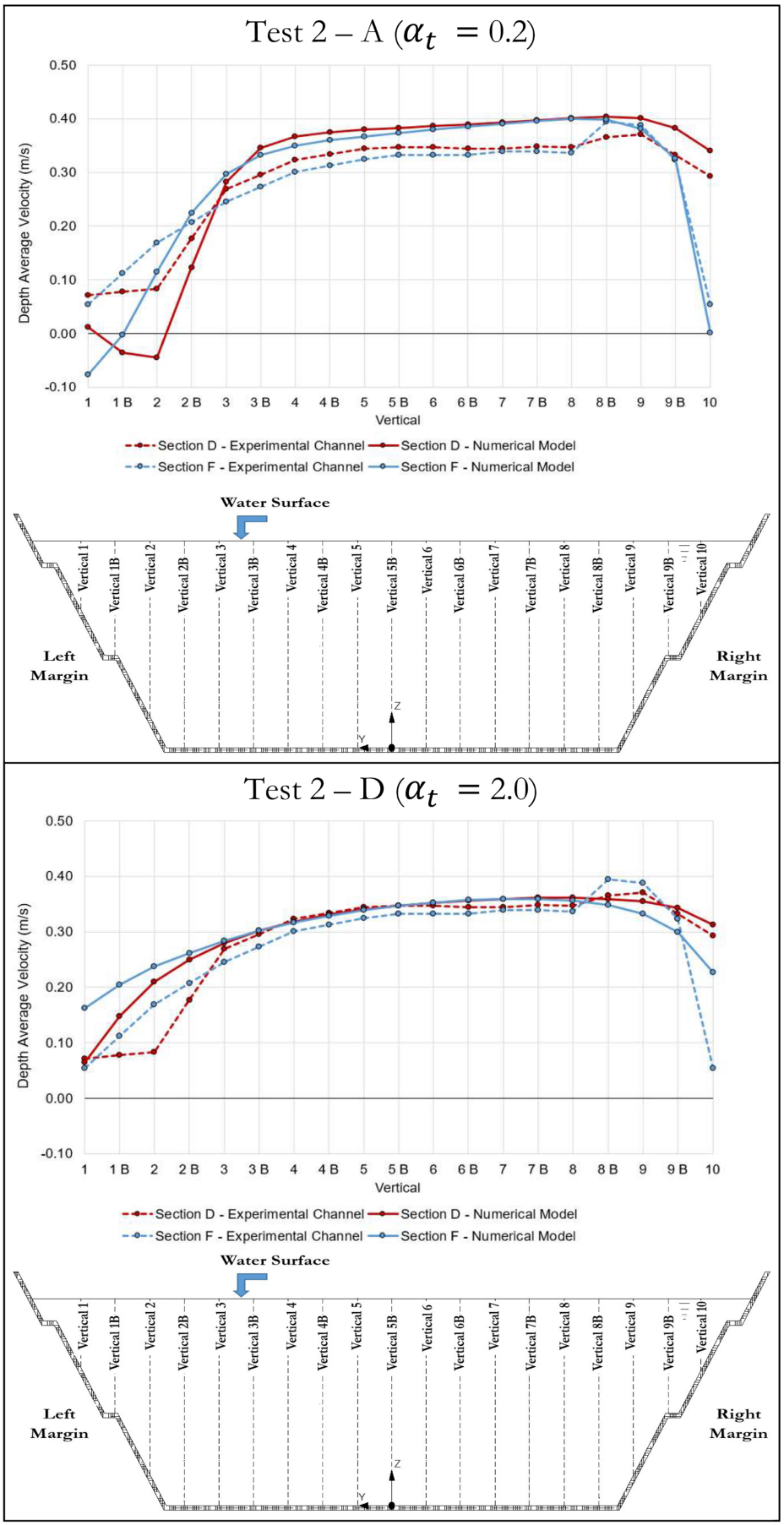


**Figure 13.** Test 2 – Depth average velocity.

The flow velocity field obtained from the numerical simulation is shown in Figure 14. A great similarity can be observed between the simulated and experimental flow field, since in both, the existence of two zones of circulations caused by separations in the regions of the curves is verified. Figure 15 shows that the numerical model was able to reproduce the general behavior of the flow and the depth average velocities at the cross sections D and F.

Table 7 presents a summary of the statistical evaluations performed in order to characterize the deviations in the velocity field. The simulation made with the model $K-\varepsilon$ presented an average percentage error (MPE) of 4.47%, being the absolute mean error of 3.1 cm/s. The efficiency coefficient of Nash-Sutclife (NSE) was equal to 0.77 which makes it possible to characterize the model as very good. It is noteworthy that the Nash-Sutclife coefficient for sections A results below 0.5. This behavior can be interpreted as a numerical distortion, since this coefficient uses the variance of the measurements as normalizing factor. This means that for the sections where the flow is more homogeneous, as is the case of section A, small errors can lead to a more unfavorable coefficient when compared to sections that present greater variations of velocity along the cross section.

## DISCUSSION OF THE RESULTS

For Test 1, which compared the simulations performed with constant turbulent viscosity model, it was observed that the simulation 1-C, which used the value of 0.005 m²/s, was the one that led to the lowest distortions in relation to the velocity field observed in the experimental channel. From the point of view of the statistical evaluations, this simulation was the one that presented the best results among all performed cases in this study, including those that used more sophisticated turbulence models, such as the $K-\varepsilon$ model. It is worth noting that the simulation 1-B, which used the turbulent viscosity of 0.01 m²/s, also led to consistent results. It is noteworthy that the turbulent value found to be the most adherent to the experimental data ($\nu_t$ = 0.005 m²/s) is larger than the theoretically estimation, that is of the order of $10^{-3}$ m²/s. A possible explanation for this is that the flow in the experimental channel is at the smooth-rough transition zone regime, which may induce a higher viscosity. Another possible explanation is that the 2D simulation (depth average flow) is unable to reproduce all

**Table 7.** Test 3 – Statistical characterization.

| Position | Statistical evaluation | | | |
|---|---|---|---|---|
| | MPE (%) | AAPE (%) | MAE (m/s) | NSE |
| Section A | 12.80 | 12.80 | 0.033 | 0.20 |
| Section B | 7.03 | 10.68 | 0.027 | 0.64 |
| Section C | -5.26 | 21.53 | 0.029 | 0.92 |
| Section D | -4.67 | 19.65 | 0.032 | 0.94 |
| Section E | 1.69 | 14.97 | 0.030 | 0.92 |
| Section F | 11.49 | 15.79 | 0.030 | 0.91 |
| Section G | 8.23 | 13.44 | 0.035 | 0.87 |
| Maximum | 12.80 | 21.53 | 0.035 | 0.94 |
| Average | 4.47 | 15.55 | 0.031 | 0.77 |
| Minimum | -5.26 | 10.68 | 0.027 | 0.20 |

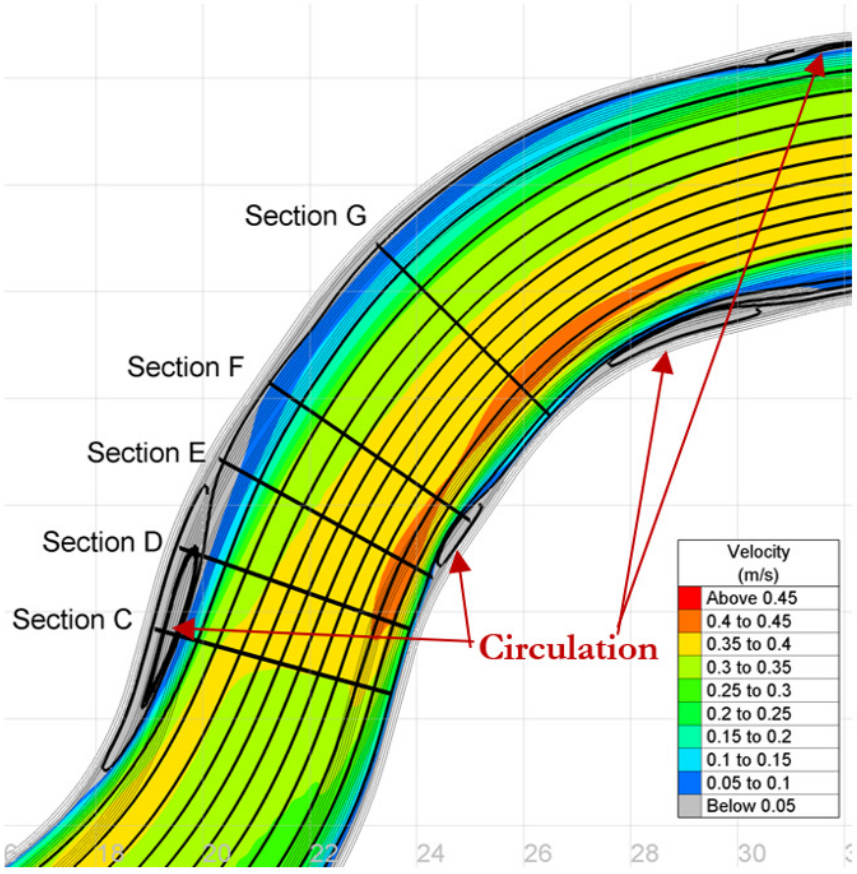


**Figure 14.** Test 3 – Streamlines.

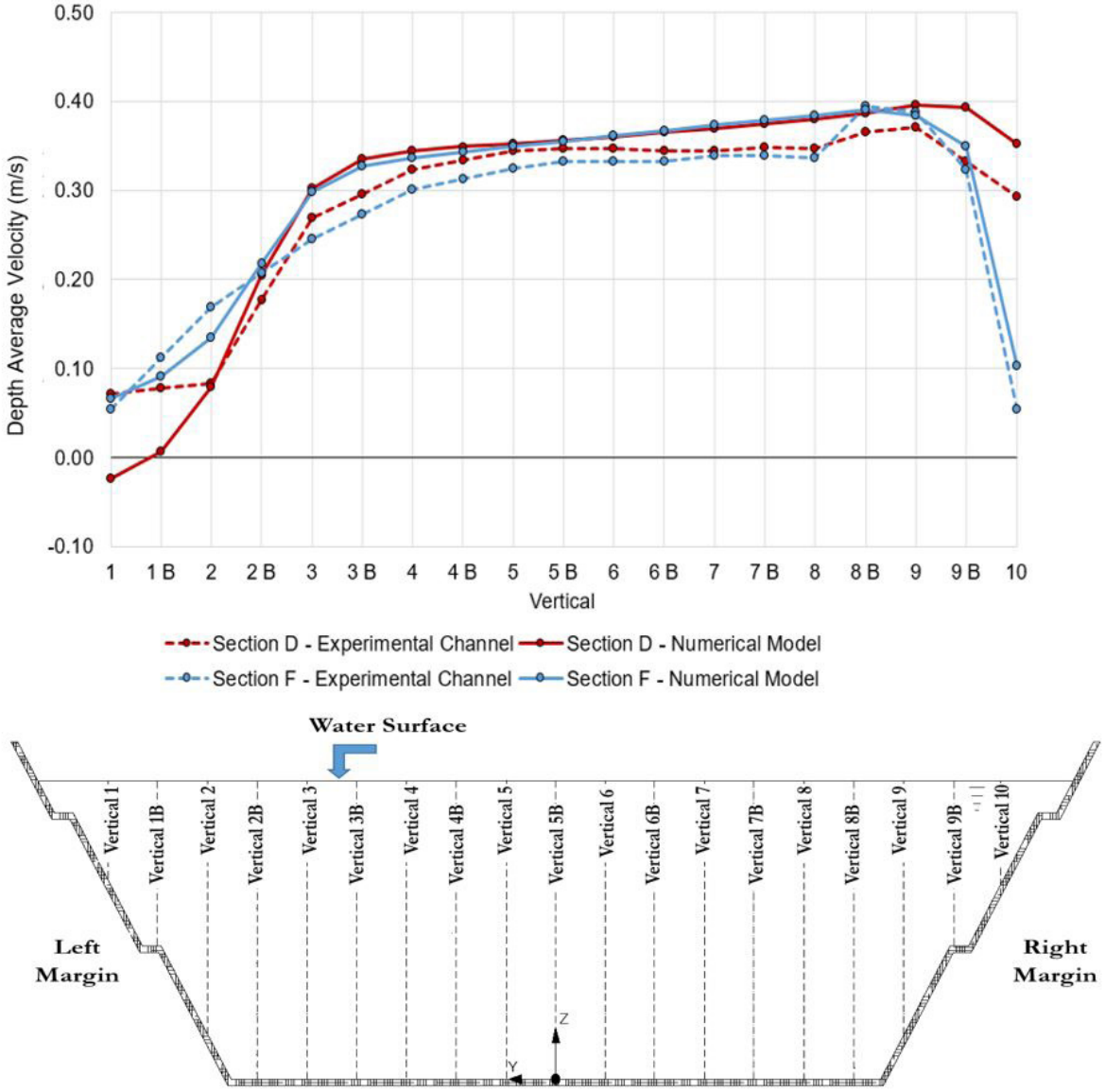


**Figure 15.** Test 2 – Depth average velocity.

the turbulent structure of a complex flow like the one observed in the experimental channel. This limitation may lead to the use of a greater turbulent viscosity in order to obtain good results.

Another important factor to note is that two-dimensional simulations do not allow the correct reproduction of the secondary currents which occur in the region of the curves, as described by Nezu & Nakagawa (1993). The existence of these secondary currents tends to induce a greater diffusivity to the flow.

As expected, the more sophisticated turbulence model ($K-\varepsilon$ model) had good results. This model allowed the reproduction of the velocity field in a suitable way for most of the computational domain because it allows the transport of the turbulent kinetic energy and the dissipation of this energy along the computational domain (Wilcox, 1994). This means that the simulated velocity field is suitable in all sections.

Despite the good general performance, the largest error observed in this simulation occurred in the region of the largest separations, that is, downstream of curve 1, near the left margin. In this region, the simulated circulation was more intense than that verified experimentally. This behavior may be related to the limitation of the experimental data, that didn´t measure the superficial layer of the flow. Another possible cause of this distortion in the numerical model is the fact that the simulations did not reproduce the secondary currents. The increment at turbulent viscosity induced by these secondary currents, generated by the anisotropy of the Reynolds tensions, could not be reproduced by $K-\varepsilon$ model, which, by definition, is isotropic (Eiger, 1989).

Among the turbulence models verified in this work, the only one that has anisotropic characteristics is Elder Model. Although it has a reasonably simple formulation, which uses algebraic equations in its formulation, this model has the capacity to divide the turbulence into two parcels, one of them being transversal to the flow and the other longitudinal. By doing so, Elder Model allows the use of different dispersion coefficients for each component, allowing the imposition of an anisotropic turbulence in the simulation. However, in spite of this clear

advantage in comparison to the other models, Elder Model proved to be less efficient than $K-\varepsilon$ model and even constant viscosity model. This was due to, in order to impose coefficients that best reproduce the circulations in the region of the curves, the velocity field in the other regions presenting distortions when compared to the experimental data. Therefore, the simulations made with this model did not allow the reproduction, at the same time and the best possible way, of the various characteristics of the flow existing along the channel.

From the tests performed with Elder Model, it was verified that the characteristics of the circulations and separations zones is heavily influenced by the transverse dispersion coefficient. As suggested by Wilson et al. (2002), the best results were obtained from the simulation 2-B, performed with the coefficient $\alpha_t = 0.6$. It should be noted, however, that the use of this dispersion coefficient caused a separation zone with more intense circulations then the experimental data, mainly in the region of the sections C, D and E, near the left margin of the channel.

All the simulations presented in this work, with the exception of the simulation 1-A, performed with the constant viscosity model with the value of $\nu_t = 0.1$ m$^2$/s, presented water levels similar to those obtained in the experimental channel (Figure 16). This shows that, in spite of the clear difference between the velocity field obtained in the simulations, mainly in terms of dimensions and intensity of the circulations, the head loss due to the friction was not significantly affected by the turbulence models.

In terms of computational time, as shown in Table 8, the model that presented the best performance was the Elder Model. This table shows the average number of steps in a 1 hour simulation. The number of steps required for each simulation was approximately 200,000. As a reference, the characteristics of the computer used to perform the simulations are shown in Table 9.

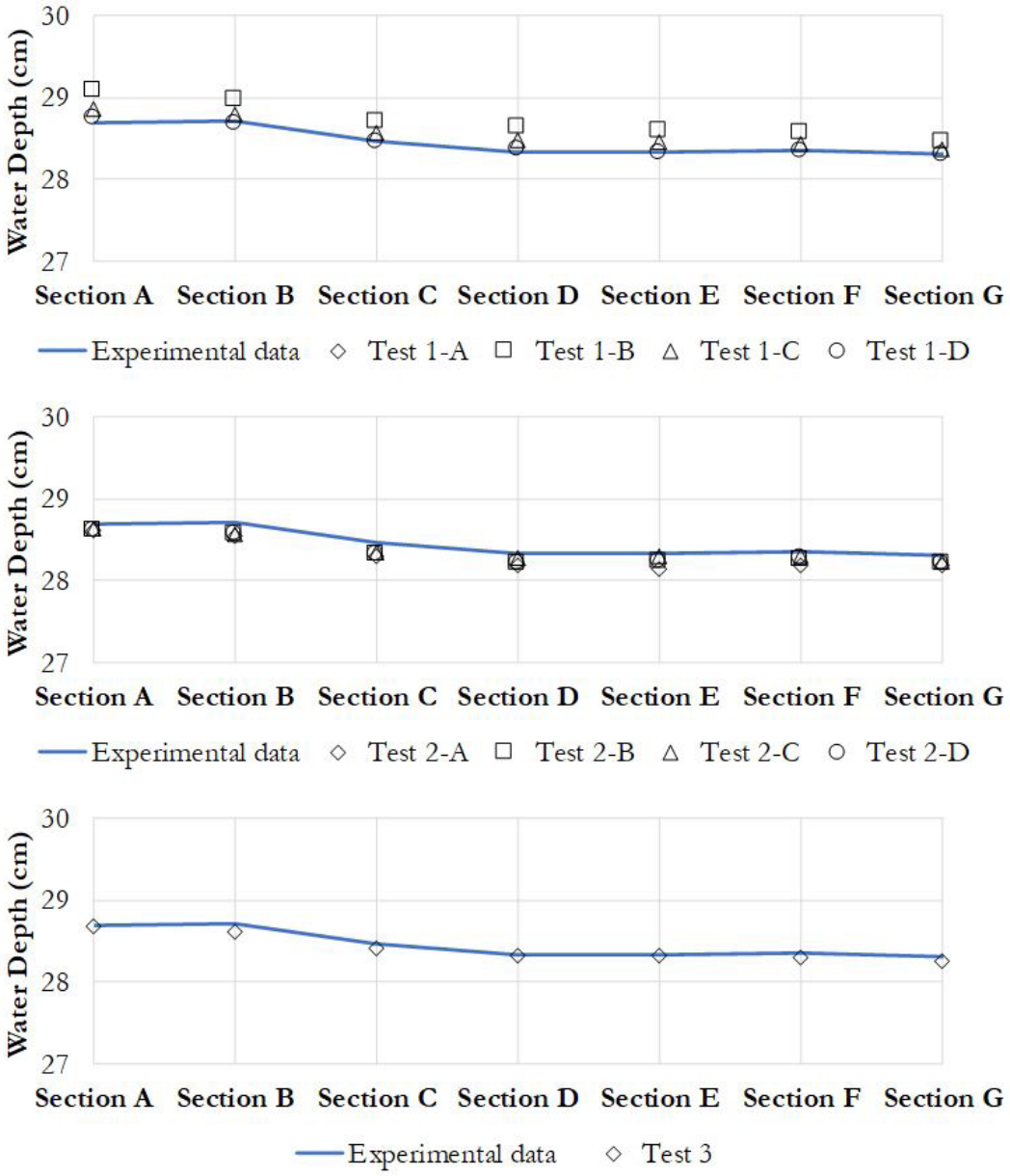


**Figure 16.** Water depth – Experimental x Simulations.

**Table 8.** Computational time.

| Turbulence model: | Simulation speed |
|---|---|
| Constant viscosity model: | 8,000 steps / hour |
| Elder Model: | 11,600 steps / hour |
| $k-\varepsilon$ Model | 8,100 steps / hour |

**Table 9.** Computer characteristics.

| Item | Characteristics |
|---|---|
| CPU | Intel® Core i7-4790K – 4.00GHz |
| RAM: | 16.0GB |
| Operational Sistem | Windows® 10 Pro – 64 Bits |
| Number of cores used: | 8 cores |

## CONCLUSIONS

This paper has the main objective of contributing to the understanding of the phenomenon of turbulence and to explore how the turbulence models affect the general behavior of the simulated flow. To achieve this objective, a comparative study was carried out between the results obtained in two-dimensional computational numerical simulations performed with three different turbulence models available in the Telemac 2D standard programming. The flow velocity fields obtained in these simulations were compared with experimental data from the study developed by Yamakawa (2015).

The main focus of these comparisons was the velocity field in the region of the channel curves. These comparisons were made by statistical tests that intended to quantify the differences between the velocity fields obtained in the simulations and those observed in the experimental channel. The focus of this study in the velocity field in the region of the curves is justified because a proper implementation of a turbulence model is necessary for the correct reproduction of the separations and circulation zones. The basic hypothesis is that the use of more sophisticated turbulence models, with two transport differential equations in their formulation, leads to better results when compared to simpler models.

In total, nine simulations were performed, four with the constant turbulent viscosity model, four with Elder type model and one with $k-\varepsilon$ model.

The results obtained in this research allowed the following conclusions:

- In general, it has been observed that all verified turbulence models, when properly configured, reproduce satisfactorily the observed flow;
- However, the results showed that the simulation performed with the constant viscosity model, with the value of 0.005 m²/s, was the one with better result. This simulation presented little superior performance than the simulation performed with $K-\varepsilon$ model;
- Although constant viscosity model showed good adherence with the experimental data, the proper choice of the turbulent viscosity to be adopted is not simple, once the value found to be the most suitable for the studied flow differs significantly from the theoretical evaluations made from mixing length turbulence model ($10^{-3}$ m²/s). This difference occurs because the general characteristics of the channel and the flow itself may cause a substantially greater turbulent diffusion than theoretically estimation;
- In this sense, $K-\varepsilon$ model has the advantage of having such a small variation in its empirical coefficients that most of the researchers consider that it does not need calibration;
- Elder type model was less efficiency than the others, despite being the only one to have anisotropic characteristics. This happens because the imposition of dispersion coefficients that leads to a proper flow patterns in the region of the curve induces distortions on the velocity field in the other regions. Therefore, the simulations made with this model did not allow the reproduction, at the same time and in the best possible way, of the various characteristics of the flow existing along the channel;
- In general, it has been observed that the configuration of the turbulence models in order to impose higher values of turbulent viscosity tends to cause a decrease in the intensity and dimensions of the circulations in the region of the curves. In extreme cases, it was verified that the circulations were not formed. On the other hand, the decrease of the turbulent viscosity leads to larger circulation zones, which can, in extreme cases, cause instability in the flow, (the circulations change size and intensity constantly, preventing the occurrence of steady-state flow). Although expected, this behavior is not always well understood by users of the turbulence models;
- The obtained results showed that due to the fact that the 2D model cannot reproduce the secondary currents that occur in the region of the curves, all the turbulence models presented some limitation, underestimating the diffusion in those places. For constant turbulent viscosity model and Elder model, this limitation can be compensated by the artificial increase of the turbulent viscosity. This procedure, however, prejudice the reproduction of the flow in the other location not affected by the secondary currents, unless a more sophisticated spatial variable turbulent viscosity is imposed.

## REFERENCES

Blanckaert, K., & Vriend, H. J. (2003). Secondary flow in sharp open-channel bends. *Journal of Fluid Mechanics*, *498*, 353-380. http://dx.doi.org/10.1017/S0022112003006979.

Booij, R. (2003). Measurements and large eddy simulations of the flows in some curved flumes. *Journal of Turbulence*, *4*, 4. http://dx.doi.org/10.1088/1468-5248/4/1/008.

Canadian Hydraulics Centre – CHC. (2009). *Hydrodynamic model of St. Clair River with Telemac-2D.* Ottawa, Ontario: CHC.

Canadian Hydraulics Centre – CHC. National Research Council (2010). *Blue Kenue – Reference Manual.* Ottawa, Ontario: CHC.

Demuren, A., & Rodi, W. (1984). Calculation of turbulence-driven secondary motion in non-circular ducts. *Journal of Fluid Mechanics*, *140*, 189-222. http://dx.doi.org/10.1017/S0022112084000574.

Eiger, S. (1989). Modelos de escoamentos turbulentos. In R. C. V. Silva (Ed.), *Métodos numéricos em recursos hídricos*. (Coleção da ABRH – Associação Brasileira de Recursos Hídricos, Vol. 1, Cap. 2, pp. 84-155). São Paulo: ABRH.

Elder, J. W. (1959). The dispersion of marked fluid in turbulent shear flow. *Journal of Fluid Mechanics*, *5*(04), 544-560. http://dx.doi.org/10.1017/S0022112059000374.

Friedrich, M. F. (2004). *Aplicação de modelagem física e computacional a um escoamento fluvial* (Dissertação de mestrado). Programa de Pós-graduação em Engenharia de Recursos Hídricos e Ambientais, Universidade Federal do Paraná, Curitiba.

Gholami, A., Akbar Akhtari, A., Minatour, Y., Bonakdari, H., & Javadi, A. A. (2014). Experimental and numerical study on velocity fields and water surface profile in a strongly-curved 90º Open Channel Bend. *Engineering Applications of Computational Fluid Mechanics*, *8*(3), 447-461. http://dx.doi.org/10.1080/19942060.2014.11015528.

Hervouet, J.-M. (2007). *Hydrodynamics of free surface flows - modelling with the finite element method*. Chichester: John Willey $ Sons Ltd.

Launder, B. E., & Spalding, D. B. (1972). *Mathematical models of turbulence*. London: Academic Press.

Launder, B. E., Morse, A., Rodi, W., & Spalding, D. B. (1973). *Prediction of free shear flows: a comparison of the performance of six turbulence models* (Vol. 1). USA: NASA Official.

Moriasi, D. N., Arnold, J. G., Van Liew, M. W., Bingner, R. L., Harmel, R. D., & Veith, T. L. (2007). Model evaluation guidelines for systematic quantification of accuracy in watershed simulations. *American Society of Agricultural and Biological Engineer*, *50*, 885-900.

Nash, J. E., & Sutcliffe, J. V. (1970). River flow forecasting through conceptual models part I: a discussion of principles. *Journal of Hidrology*, *10*(3), 282-290. http://dx.doi.org/10.1016/0022-1694(70)90255-6.

Nezu, I., & Nakagawa, H. (1993). *Turbulence in open-channel flows*. Rotterdam: A.A.Balkema.

Pope, S. B. (2000). *Turbulent flows*. Cambridge: Cambridge University Press. http://dx.doi.org/10.1017/CBO9780511840531.

Schlichting, H. (1968). *Boundary-Layer theory* (6th ed.). New York: McGraw-Hill Book Company, Inc..

Van Balen, W., Uijttewaal, W. S. J., & Blanckaert, K. (2009). Large-eddy simulation of a mildly curved. *Journal of Fluid Mechanics*, *630*, 413-442. http://dx.doi.org/10.1017/S0022112009007277.

Wilcox, D. C. (1994). *Turbulence Modeling for CFD* (2nd ed.). La Cañada: DCW Industries, Inc..

Wilson, C. A. M. E., Bates, P. D., & Hervouet, J. M. (2002). Comparison of turbulence models for stage-discharge rating curve prediction in reach-scale compound channel flows using two-dimensional finit element methods. *Journal of Hydrology (Amsterdam)*, *257*(1-4), 42-58. http://dx.doi.org/10.1016/S0022-1694(01)00553-4.

Yamakawa, F. H. S. (2015). *Estrutura do escoamento em canais trapezoidais em curva* (Dissertação de mestrado). Programa de Pós-graduação em Engenharia de Recursos Hídricos e Ambientais, Universidade Federal do Paraná, Curitiba.

## Authors contributions

José Rodolfo Machado de Almeida: Literature review, development and application of the methodology, analysis of the results and discussion of the results.

José Junji Ota: Development of the methodology, analysis of the results and discussion of the results.